Publ. Astron. Soc. Japan (2016) 68 (3), L5 (1–5)
doi: 10.1093/pasj/psw017
Advance Access Publication Date: 2016 March 17
Letter

Letter

Transiting planets as a precision clock to constrain the time variation of the gravitational constant

Kento Masuda[1,*] and Yasushi Suto[1,2]

[1]Department of Physics, The University of Tokyo, 7-3-1 Hongo, Bunkyo-ku, Tokyo 113-0033, Japan
[2]Research Center for the Early Universe, School of Science, The University of Tokyo, 7-3-1 Hongo, Bunkyo-ku, Tokyo 113-0033, Japan

*E-mail: masuda@utap.phys.s.u-tokyo.ac.jp

Received 2015 December 28; Accepted 2016 February 5

Abstract

Analysis of transit times in exoplanetary systems accurately provides an instantaneous orbital period, $P(t)$, of their member planets. A long-term monitoring of those transiting planetary systems puts limits on the variability of $P(t)$, which are translated into the constraints on the time variation of the gravitational constant G. We apply this analysis to 10 transiting systems observed by the Kepler spacecraft, and find that $\Delta G/G \lesssim 5 \times 10^{-6}$ for 2009–2013, or $\dot{G}/G \lesssim 10^{-6}\ \mathrm{yr}^{-1}$ if $\dot{G}$ is constant. While the derived limit is weaker than those from other analyses, it is complementary to them and can be improved by analyzing numerous transiting systems that are continuously monitored.

Key words: gravitation — planets and satellites: general — techniques: photometric

1 Introduction

Are the fundamental *constants* in nature really *constant* over the cosmological time scale? This question has a long history in physics and cosmology, and has been discussed intensively in different contexts. One of the most famous examples includes the Large Number Hypothesis by Dirac (1937), who raises a possibility of the gravitational constant G being proportional to t^{-1}.

Recently, Anderson et al. (2015) reported a curious oscillatory trend in the values of G measured over the last three decades, $\Delta G/G \approx 2.4 \times 10^{-4} \sin[2\pi t/(5.9\,\mathrm{yr})] + \mathrm{const.}$]. More intriguingly, they claimed that the period and phase of the modulation are in agreement with the variation of the length of a day of the Earth (Holme & de Viron 2013; Speake & Quinn 2014). The proposed modulation, however, is unlikely to reflect the real-time variation of G (Anderson et al. 2015). Indeed, the amplitude of ΔG is shown to be inconsistent with the dynamics of the solar system (Iorio 2016). In addition, the subsequent studies (Schlamminger et al. 2015; Pitkin 2015; Scholkmann & Sieber 2016, and added appendix of Anderson et al. 2015) have shown that the trend reported by Anderson et al. (2015) is more likely to be an artifact. Nevertheless, it is important and interesting to discuss and compare with other independent constraints on ΔG on such short time scales since most of the previous literature has focused on ΔG averaged over the cosmological time scale.

For that purpose, we consider the orbital periods of transiting exoplanetary systems in the present paper. So far, more than 4000 candidate systems have been reported by the Kepler mission (Mullally et al. 2015), which have

been monitored over several years, and approximately 1000 of them have been confirmed to host planets. The orbital period P of such planets can be accurately determined by their central transit times. Furthermore, a systematic search for any time variability of the period has been performed primarily in order to probe the gravitational interaction between multiple planets, which is referred to as the transit timing variation (TTV: Agol et al. 2005; Holman & Murray 2005).

The TTV analysis is conventionally used to determine the mass of planets without radial velocity follow-up observations and/or to infer the presence of undetected perturbers. Instead, we attempt to put a constraint on the time variation of G from the same analysis, but focusing on those systems that exhibit no clear TTV signature. In particular, *hot Jupiters*, planets orbiting around host stars within a week or so, are particularly suited for constraining the variation of G on time scales of months to years.

As will be shown below, our sample yields the constraint $\dot{G}/G \lesssim 10^{-6}\,\mathrm{yr}^{-1}$ *if* $\dot{G}$ *is constant*, which is weaker by six orders of magnitude than those based on the pulsar timing (e.g., Williams et al. 1976; Kaspi et al. 1994; Zhu et al. 2015) and the lunar ranging (e.g., Hofmann et al. 2010). We would like to emphasize, however, that the conventional assumption of the constant $\dot{G}$ is not general, but has been introduced just for simplicity. If G did vary periodically as was claimed by Anderson et al. (2015), planetary systems with different orbital periods would be ideal to search for the possible resonant effect close to the variation period of days to years, and thus the resulting constraint on the amplitude of $\dot{G}$ could be stronger depending on the expected period of the oscillation. Therefore it would be interesting to know the current limit from the existing systems at this point in any case.

The precise data of our solar system also put more stringent constraints on the variation of G, but they are mostly sensitive to the variability on time scales of years, and the perturbative effect of eight planets and other bodies need to be carefully separated, as has been performed by Iorio (2016), for instance. On the contrary, the result from different transiting systems can be simply added for tighter constraints because the effect of ΔG should change the period of any system in a coherent fashion. For these reasons, TTVs of transiting planetary systems offer a complementary and straightforward method to explore the variation of G on shorter time scales.

2 Transit timing variation analysis of planetary systems

In the two-body problem, motion of a planet around its host star is exactly periodic, and so are its transits. The transit times of a planet in a multiple planetary system; however, sometimes deviate from the exact periodicity due to the gravitational perturbation from other planets in the system. This phenomenon, known as the "transit timing variation" (TTV: Agol et al. 2005; Holman & Murray 2005), has been successfully modeled in tens of multi-transiting planetary systems discovered by Kepler to determine the mass ratios of their member planets (e.g., Holman et al. 2010; Lissauer et al. 2011; Masuda 2014) as well as to infer the existence of non-transiting planets (e.g., Nesvorný et al. 2012; Masuda et al. 2013).

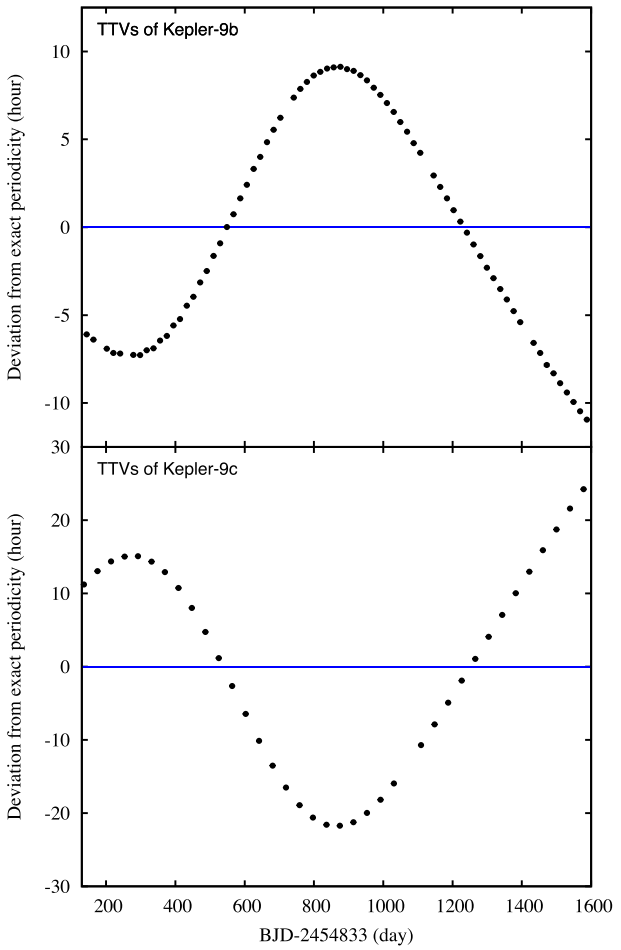

Fig. 1. TTVs in the Kepler-9 system, where two planets near a 2 : 1 mean motion resonance (Kepler-9b with $P = 19.3$ d, top; Kepler-9c with $P = 38.9$ d, bottom) transit the same host star. The residuals of the transit times from the linear fit are plotted against the Kepler observational time spanning about four years. The error of each transit time is smaller than the point size. (Color online)

Figure 1 displays an example of the TTV signals for the Kepler-9 system, which is the first multiple planetary system detected through the transit method. It hosts two transiting planets, Kepler-9b ($0.137\,M_{\mathrm{Jup}}$) and Kepler-9c ($0.094\,M_{\mathrm{Jup}}$) with orbital periods of 19.3 d and 38.9 d, respectively (Borsato et al. 2014). In this system, the orbital periods

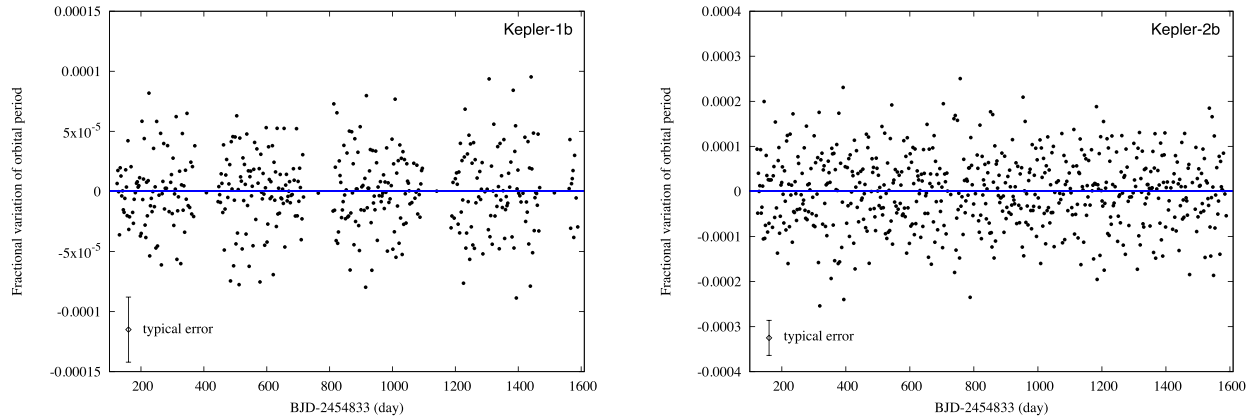

Fig. 2. $\Delta P/P$ against BJD for Kepler-1b (left) and Kepler-2b (right). (Color online)

of the two planets are not exactly constant because of the strong mutual gravitational interaction between the two, in addition to the dominant gravity due to the host star ($1.07\,M_\odot$). This results in systematic deviations of the central transit times with respect to the mean period, as exhibited by filled circles in the figure.

Such TTV signals have often been used to constrain the system parameters, in particular to estimate the mass of planets without radial velocity measurement. In the following, however, we use the *absence* of the TTV signal to put an upper limit on the period variation ΔP, which translates into ΔG through Kepler's third law:

$$P = 2\pi\sqrt{\frac{a^3}{GM}}, \tag{1}$$

where a is the semi-major axis and M is the total mass of the two-body system.

Although equation (1) is exactly correct only when G is constant, we assume that it still holds when G varies adiabatically, as we consider here. Then it leads to

$$\frac{\dot{P}}{P} = \frac{3}{2}\frac{\dot{a}}{a} - \frac{1}{2}\frac{\dot{G}}{G} - \frac{1}{2}\frac{\dot{M}}{M}. \tag{2}$$

Note that the variation of G, in principle, simultaneously induces non-vanishing $\dot{a}$ and $\dot{M}$. Thus, it may be more useful to rewrite equation (1) in terms of the specific angular momentum j and the eccentricity e:

$$P = \frac{2\pi j^3}{G^2M^2(1-e^2)^{3/2}}. \tag{3}$$

Then we have

$$\frac{\dot{P}}{P} = 3\frac{\dot{j}}{j} - 2\frac{\dot{G}}{G} - 2\frac{\dot{M}}{M}. \tag{4}$$

Equation (4) simply reduces to

$$\frac{\dot{P}}{P} = -2\frac{\dot{G}}{G}, \tag{5}$$

if the orbit is circular and both the specific angular momentum and mass are conserved under the variation of G (e.g., Uzan 2003). While the assumption of $\dot{M} = 0$ is perfectly justified for non-relativistic stars and planets considered here, it is not the case for compact objects including neutron stars.

2.1 Constraints from individual systems: Kepler-1 and Kepler-2

Among the confirmed transiting planets observed with Kepler, we select Kepler-1b (or TrES-2) with $1.20\,M_{\rm Jup}$ and a 2.47-d period, and Kepler-2b (or HAT-P-7b) with $1.78\,M_{\rm Jup}$ and 2.20-d period. The two planets have the highest transit signal-to-noise ratio, while exhibiting no identifiable feature of TTVs. In figure 2, we show the fractional variations in the orbital periods of these planets against the observed date. For each planet, we follow the procedure of Masuda (2015) to determine the central times of individual transits t_i, where i stands for the number of transits counted from a fixed epoch. Here we use only the data sampled at a short cadence (one minute), which yield the transit times with higher precision than the long cadence data sampled at the 30-minute interval. We compute the orbital period P_i between t_i and t_{i+1} for each i and plot $(\Delta P/P)_i \equiv (P_i - \overline{P})/\overline{P}$ against $(t_{i+1} + t_i)/2$, where $\overline{P}$ is an average of all P_i. The corresponding root-mean-square $\Delta P/P$ are 3×10^{-5} and 8×10^{-5} for Kepler-1b and Kepler-2b, respectively. These values translate into $\Delta G/G = 1.5 \times 10^{-5}$ and 4×10^{-5} over four years, which are smaller than the amplitude of the proposed variation of G (Anderson et al. 2015) by an order of magnitude.

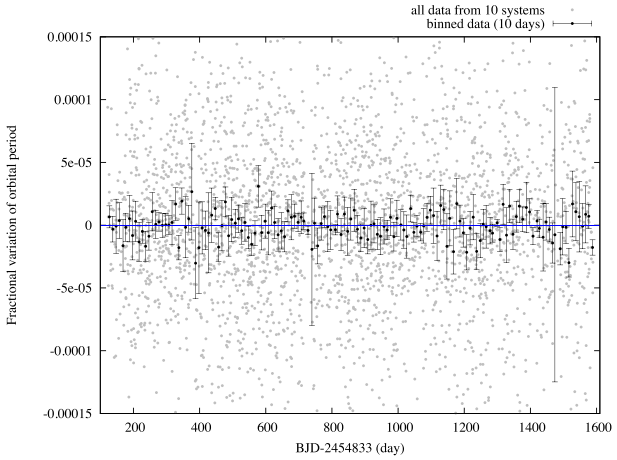

Fig. 3. $\Delta P/P$ against BJD for the 10 transiting systems analyzed in section 2.2. The gray dots are all the data points, while the black circles with error bars are those averaged into 10-day bins. (Color online)

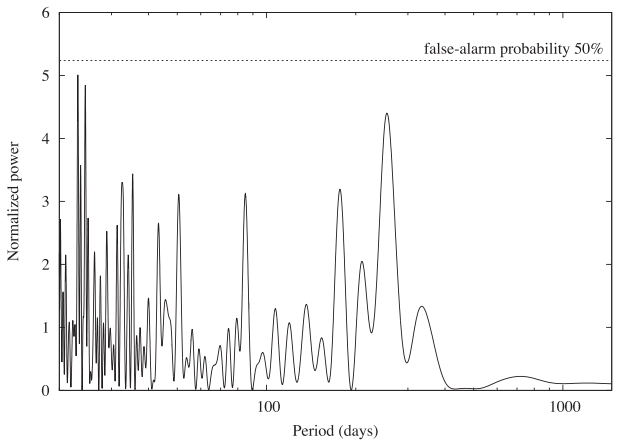

Fig. 4. Lomb–Scargle periodogram (Scargle 1982) of the binned data in figure 3. The vertical axis is normalized to the variance of the data. The horizontal dashed line indicates the power level corresponding to the false-alarm probability (significance level) of 50%; this is the probability that any of the peaks exceeds a given power level when the data points are independent Gaussians.

2.2 Constraint from a statistical sample

The constraints from the above two systems almost reach the limit of the Kepler photometry for the existing systems. However, the further improvement can be achieved by combining many systems in a statistical fashion. We select 10 confirmed transiting planetary systems with the highest transit signal-to-noise ratios: Kepler-1, Kepler-2, Kepler-13, Kepler-12, Kepler-6, Kepler-7, Kepler-423, Kepler-17, Kepler-5, and Kepler-3. None of these systems exhibit any clear TTVs. Although the transit times in some of these systems (e.g., Kepler-3 or alias HAT-P-11) are affected by the strong star-spot activities that deform the transit signals, we do not exclude them because our purpose here is simply to illustrate the advantage of combining the constraints from many independent systems.

We apply the same analysis as in the previous subsection to the above 10 systems. We plot the resulting $\Delta P/P$ as gray dots in figure 3, and their averages in 10-day bins as black circles with error bars. Now the standard deviation of the binned $\Delta P/P$ is 1×10^{-5}, which is a few times smaller than the constraints from the individual systems. Note that the choice of the smoothing bin size is completely arbitrary at this point. The binning would smooth out a possible variation of G less than the bin size and the resulting $\Delta P/P$ would depend on the bin size. Here we choose the 10-day bin just for definiteness, and could use a different value if a specific model of the variation of G is given.

The periodogram of the binned $\Delta P/P$ in figure 4 delivers a rough idea of the expected constraints for the different choice of the smoothing bin size.[1] All of the peaks in the periodogram have amplitudes less than the significance level of 50% (horizontal dashed line) and are consistent with the Gaussian noise, i.e., the data exhibit no significant modulation over the period range down to $\sim$10 d. A larger bin size therefore should put a somewhat stronger constraint on $\Delta P/P$, and hence on $\Delta G/G$. The proper interpretation of the constraint, however, depends on the model of $G(t)$.

[1] We made use of the pyTiming module of PyAstronomy ⟨https://github.com/sczesla/PyAstronomy⟩ to compute the periodogram.

3 Conclusion and discussion

We have shown that the methodology of using exoplanets as a precision clock provides reasonably interesting limits on the time variation of G. Our current analysis finds $\Delta G/G \lesssim 5 \times 10^{-6}$ for 2009–2013, which corresponds to $\dot{G}/G \lesssim 10^{-6}\ \mathrm{yr}^{-1}$ if $\dot{G}$ is constant. In contrast, constraints from Lunar Laser Ranging experiments and the binary pulsar system PSR B1913+16 correspond to $\dot{G}/G < 8 \times 10^{-12}\ \mathrm{yr}^{-1}$ (Williams et al. 1996) and $\dot{G}/G = (4 \pm 5) \times 10^{-12}\ \mathrm{yr}^{-1}$ (Kaspi et al. 1994), respectively.

Although our current constraint is significantly less stringent than the binary pulsar timing result that is based on the similar principle, it is complementary in many aspects. First, we can safely neglect $\dot{M}$ for exoplanetary systems unlike binary pulsar systems where the self-gravitational energy significantly contributes to the total mass. Secondly, we may constrain the $\dot{a}$-term independently of $\dot{P}$ by combining the precise measurement of the radial velocity (proportional to a/P) with the photometric transit timing data. Thirdly, the timing analysis of the secondary eclipse (opposite phase of the planetary transit in front of the host star, i.e., the occultation of the planet by the stellar disk) of transiting

planets may also constrain the $\dot{a}$-term through the variation of the expected arrival time difference $\approx a/c$ from the photometric data alone. Fourthly, the growing number of continuously monitored transiting planets promises to improve statistically the constraint beyond the value that we discuss in this paper. Incidentally, if G varies periodically with an oscillation period of days to years, the dynamics of the planetary system with a similar orbital period would be perturbed in a resonant fashion. While we have not studied such a possible resonant effect in this paper, constraints from systems with different periods are important once the simple assumption of a constant $\dot{G}$ is abandoned.

Finally, we would like to emphasize that the current data for numerous exoplanetary systems are already precise enough to put complementary and meaningful constraints on the variation of the fundamental constants, as has been feasible only through the solar system data and/or a few binary pulsars. Thus future data of the exoplanetary systems should definitely improve the situation and might even bring an unexpected surprise.

Acknowledgments

We thank Teruaki Suyama for calling our attention to Anderson et al. (2015). K.M. is supported by Japan Society for the Promotion of Science (JSPS) Research Fellowships for Young Scientists (No. 26-7182), and also by the Leading Graduate Course for Frontiers of Mathematical Sciences and Physics. Y.S. acknowledges the support from the Grant-in Aid for Scientific Research by JSPS (No. 24340035).

References

Agol, E., Steffen, J., Sari, R., & Clarkson, W. 2005, MNRAS, 359, 567
Anderson, J. D., Schubert, G., Trimble, V., & Feldman, M. R. 2015, Europhysics Lett., 110, 10002
Borsato, L., Marzari, F., Nascimbeni, V., Piotto, G., Granata, V., Bedin, L. R., & Malavolta, L. 2014, A&A, 571, A38
Dirac, P. A. M. 1937, Nature, 139, 323
Hofmann, F., Müller, J., & Biskupek, L. 2010, A&A, 522, L5
Holman, M. J., et al. 2010, Science, 330, 51
Holman, M. J., & Murray, N. W. 2005, Science, 307, 1288
Holme R., & de Viron O.2013, Nature, 499, 202
Iorio, L. 2016, Classical Quantum Gravity, 33, 045004
Kaspi, V. M., Taylor, J. H., & Riba, M. F. 1994, ApJ, 428, 713
Lissauer, J. J., et al. 2011, Nature, 470, 53
Masuda, K. 2014, ApJ, 783, 53
Masuda, K. 2015, ApJ, 805, 28
Masuda, K., Hirano, T., Taruya, A., Nagasawa, M., & Suto, Y. 2013, ApJ, 778, 185
Mullally, F., et al. 2015, ApJS, 217, 31
Nesvorný, D., Kipping, D. M., Buchhave, L. A., Bakos, G. Á., Hartman, J., & Schmitt, A. R. 2012, Science, 336, 1133
Pitkin, M. 2015, Eur. Lett., 111, 30002
Scargle, J. D. 1982, ApJ, 263, 835
Schlamminger, S., Gundlach, J. H., & Newman, R. D. 2015, Phys. Rev. D, 91, 121101
Scholkmann, F., & Sieber, O. D. 2016, Eur. Lett., 113, 20001
Speake, C., & Quinn, T. 2014, Phys. Today, 67, 27
Uzan, J.-P. 2003, Rev. Mod. Phys., 75, 403
Williams, P. J., Newhall, X. X., & Dickey, J. O. 1996, Phys. Rev. D, 53, 6730
Zhu, W. W., et al. 2015, ApJ, 809, 41